13TH CANADIAN MASONRY SYMPOSIUM
HALIFAX, CANADA
JUNE 4TH – JUNE 7TH 2017

A COMPARISON OF EXPERIMENTAL AND ANALYTICAL RESULTS OF UNGROUTED BLOCK WALLS WITH UNBONDED REINFORCEMENT

Miranda, Henry[1]; Feldman, Lisa R.[2] and Sparling, Bruce F.[3]

ABSTRACT

Nine block wall specimens featuring conventional reinforcement placed in ungrouted cells were constructed as part of a larger experimental investigation at the University of Saskatchewan. Six of the specimens featured a fully grouted first course, with the remainder of the wall being ungrouted; the remaining three walls were completely ungrouted. The walls were tested with well-defined support conditions under monotonically increasing four-point out-of-plane loading. Preliminary results showed that these walls exhibited considerably increased ductility and load-carrying capacity as compared to unreinforced walls. Visual observations made during testing confirmed the development of a three-hinged mechanism; in addition to the pinned top support, cracks formed between the base of the wall and the supporting concrete grade beam and within the constant moment region between the points of applied load. The resulting load versus mid-height deflection response appeared to be insensitive to whether or not the first block course was grouted. An analytical model developed to predict the load versus mid-height deflection response theoretically matched reasonably well with that obtained experimentally.

KEYWORDS: *concrete block masonry, out-of-plane loading, hinge mechanism, reinforcement*

INTRODUCTION

Vertical reinforcement is generally added to concrete block masonry walls to improve their flexural capacity when subject to out-of-plane loads resulting from wind and earthquakes. Typical Canadian construction practice requires that the reinforced block cells are grouted to ensure strain compatibility between the reinforcement and the surrounding cementitious materials [1]. However, this construction practice is time consuming, expensive, increases member self-weight,

[1] Ph.D. Candidate, University of Saskatchewan, 57 Campus Drive, Saskatoon, SK, Canada, hpm916@mail.usask.ca
[2] Associate Professor, Department of Civil, Geological, and Environmental Engineering, University of Saskatchewan, 57 Campus Drive, Saskatoon, SK, Canada, lisa.feldman@usask.ca
[3] Professor, Department of Civil, Geological, and Environmental Engineering, University of Saskatchewan, 57 Campus Drive, Saskatoon, SK, Canada, bruce.sparling@usask.ca

and increases the risk of workplace injuries as it requires workers to thread blocks up and over reinforcement that has already been grouted in place unless special A- or H-shaped units are used.

Results of a proof-of-concept experimental study in progress at the University of Saskatchewan [2] has shown that ungrouted walls featuring conventional reinforcement that is not bonded to the surrounding masonry (denoted subsequently as unbonded reinforcement) have considerably increased ductility and load-carrying capacity as compared to unreinforced walls with similar geometry. Therefore, this approach appears to hold significant promise as long as methods by which they can be easily constructed in the field can be found. However, an analytical method is required to accurately predict their load-carrying capacity and lateral displacement behaviour.

Much of the published literature related to current research has focused on the out-of-plane behaviour of the masonry walls featuring prestressed or post-tensioned reinforcement, along with the development of associated analytical models. For instance, Dawe and Aridru [3] studied the effect of the prestressing force and the lateral deflection upon wall stiffness to calculate the ultimate moment of a series of walls with bonded tendons. Devalapura [4] used the actual material properties of the post-tensioned grouted and ungrouted panels and the resulting moment curvature diagrams at various stages to conceptualize with significant accuracy theoretical load versus deflection curves for those specimens. The bilinear behavior and Harton and Tadros [5] methods are also presented in this work. Graham and Page [6], based on flexural analysis, strain and stress compatibility for bonded walls and Phipp's [7] approximation for unbonded walls, calculated the ultimate capacity of masonry wall sections. Popehn et al. [8] developed a model to describe the three main response stages including crack penetration, formation of a crack and development of a plastic section, along with the resisting moment at each stage derived from a flexural analysis for specimens with two bars externally applied to brick and block walls with varying magnitudes of post-tensioning force. Due to the extremely low prestressing levels being used in the current study, though, it is unclear whether the assumption of first-order flexural behaviour underlying most of the previous work applies equally well to the walls in this study once significant cracking has taken place.

This paper presents the results of an experimental program consisting of nine ungrouted block walls featuring unbonded conventional reinforcement and compares their measured response with the results of an analytical method used to calculate their load-deflection behaviour.

EXPERIMENTAL DESIGN

Nine ungrouted block masonry walls with unbonded reinforcement were constructed as part of a larger experimental program. All specimens were 14 courses tall and were constructed with standard 200 mm concrete blocks in a running bond pattern by an experienced mason. The description of the specimens, material properties, and test setup are described in detail by Miranda et al. [2].

Specimen Details

Figure 1 shows the elevation, relevant cross-sections, and details of the wall specimens included in this study. The elevation in Figure 1 shows that all specimens were built atop 1700 mm long reinforced concrete beams. These beams extended, on either side, beyond the masonry wall above such that they could be clamped to the laboratory strong floor during testing and serve as a realistic bottom support for the specimens.

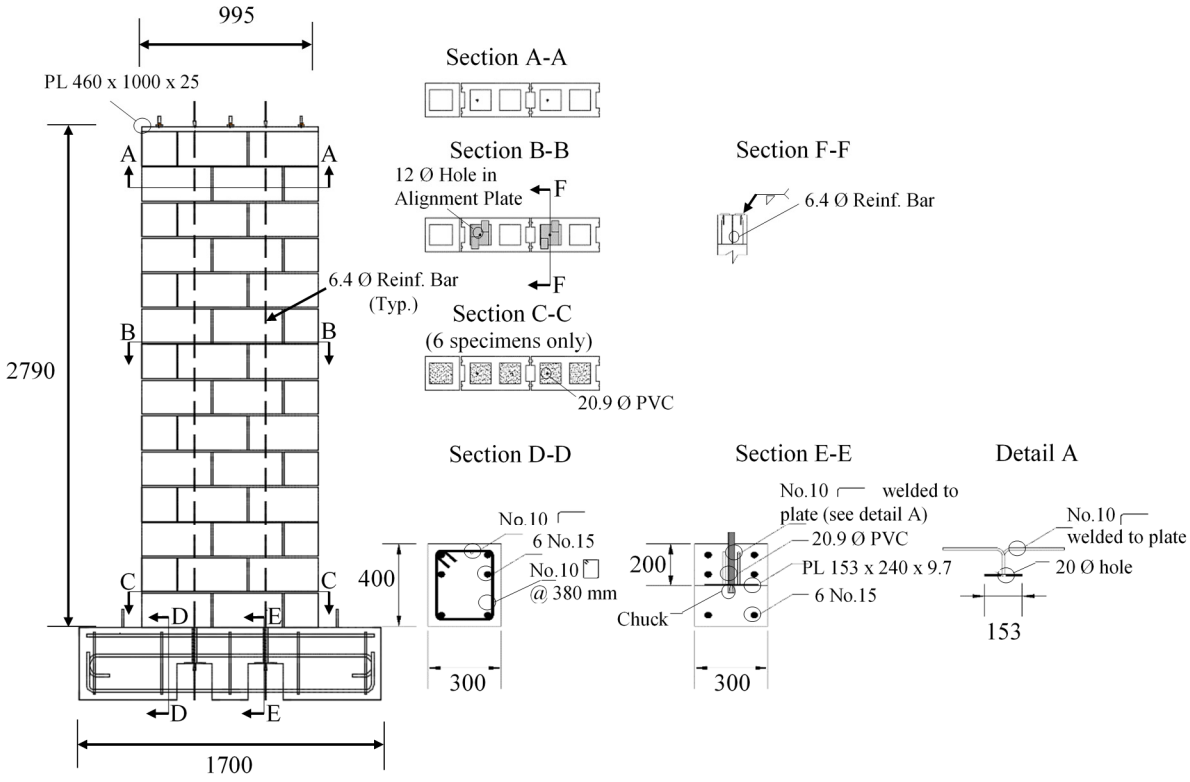

Figure 1: Wall Specimens

Section D-D in Figure 1 provides the overall cross-sectional dimensions and reinforcement for the grade beams while Section E-E provides the details of the blockouts needed to accommodate the bottom, dead end anchors for the vertical reinforcement.

Section A-A and the elevation in Figure 1 show that a single 6.4 mm diameter deformed reinforcing bar conforming to ASTM A1064/A1064M-15 [9] was placed in the first interior block cell on either side of the specimen. Sections B-B and F-F in Figure 1 show the alignment plates that were located in the bed joints above the second, sixth, eighth, and twelfth block courses to maintain the position of the reinforcing bars with respect to the compressive face of the walls and so maintain their flexural resistance during specimen loading. Guide ropes were threaded up the reinforced cells as specimens were constructed to allow the reinforcing bars to be pulled through the walls following block laying. Immediately prior to testing, the reinforcing bars were stressed

to a minimal initial load with an average magnitude of 523 N in order to ensure that the bars were straight and taut at the start of the test and to avoid any gap between the upper concrete block course and the top support assemblage. Actual stressing loads, F_{pi}, for individual specimens are shown in Table 1. Bars were anchored at the top of the wall (i.e. the live end) as shown on the elevation in Figure 1.

Table 1: Summary of Experimental Test Results

Specimen ID[a]	F_{pi} (N)	P_{cr} (kN)	Δ_{cr} (mm)	P_{max} (kN)	Δ_{max} (mm)
UB-U1	420	1.77	0.3	4.35	85.5
UB-U2	740	0.75	0.1	6.89	62.0
UB-U3	700	1.55	0.3	6.79	57.8
Mean =	620	1.15[b]	0.2[b]	n/a	n/a
COV (%) =	28.1	49.2[b]	70.7[b]	n/a	n/a
UB-G1	800	1.69	2.1	8.51	39.2
UB-G2	730	1.70	0.5	7.49	52.9
UB-G3	400	2.27	0.3	7.27	56.6
UB-G4	370	1.83	0.4	6.91	66.8
UB-G5	380	2.02	1.4	7.54	77.4
UB-G6	460	2.11	0.05	9.45	114
Mean =	523	1.94	0.8	n/a	n/a
COV (%) =	36.5	12.1	99.7	n/a	n/a

[a]The first two letters in the specimen identification identifies that they contain unbonded reinforcement (UB), the letter following the hyphen either identifies that the first block course remains ungrouted (U) or is fully grouted (G), and the number that follows identifies the replicate number within the test series.
[b]Values shown have been calculated excluding those reported for specimen UB-U1.

Section C-C in Figure 1 shows that six of the nine specimens constructed had all cells in the first block course grouted to mitigate premature web failure adjacent to the base of the wall that could develop during loading. The bottom course in the remaining three specimens was left ungrouted.

Transverse reinforcement was not provided, as was mentioned before, since it was determined that shear would not govern the design, based CAN/CSA S304.1-04 [10] provisions, even at load levels that would be expected for conventionally reinforced and grouted wall specimens of similar dimensions and reinforcing levels. Once constructed, specimens were cured in the laboratory for a minimum of 28 days prior to testing.

Material Properties

The concrete block units measured 390 mm long x 190 mm wide x 190 mm high, had frogged ends, and a nominal compressive strength of 15 MPa. Half blocks were cut from full blocks in the laboratory to ensure that all material came from a single batch. Mortar was prepared using Type S mortar cement and a 3:1 masonry-to-sand ratio. Type GU cement, aggregate with a maximum

size of 20 mm, a 5:1 aggregate-to-cement ratio by weight, and a water-to-cement ratio ranging from 0.95 to 1.00 was used to prepare the grout. Table 2 shows the results of the companion tests of cementitious materials for all specimens, as prepared and tested in conformance with the relevant standards.

The 6.4 mm diameter deformed bars used to reinforce the walls vertically had a nominal yield strength of 515 MPa. An actual yield strength of 542 (COV = 0.7%), and a measured ultimate strength of 593 MPa (COV = 0.6%), was determined by testing 7 samples of these bars in accordance with ASTM Standard A370-15 [11].

Table 2: Material Properties

Material	# of Specimens	Mean Strength (MPa)	COV (%)
Concrete Blocks	6	22.2	7.4
Mortar Cubes[a]	84	18.7	17.6
Ungrouted Masonry Prisms[b]	9	20.5[c]	8.9[c]
Bond Wrench Test[d]	9	0.06	89.9

[a]Prepared and tested in accordance with CSA Standard A3004-C2[12] at a rate of 10 kN/min

[b]Prisms were three blocks high by one block wide tested in accordance with CSA Standard S304-04 Annex D [10] at a constant loading rate of 1 kN/s.

[c]Values shown have been calculated excluding reported values for specimen UB-U1.

[d]Specimens were two blocks high by one block wide and constructed and/or tested in accordance with CSA Standard S304-04 Annex E [10].

Instrumentation and Testing

Figure 2 shows a schematic of the loading arrangement and specimen instrumentation. Figure 3 shows the top support assemblage used to approximate the guide-angle supports typically used in practice for non-load bearing walls [13]. A layer of plaster was placed between the top course of the wall and the 25 mm steel plate shown in Figure 3 to ensure uniform contact.

Figure 2 shows that a single MTS actuator with a spreader beam assembly was used to create a four-point loading arrangement for the specimens. In addition, horizontal spreader beams extended across the full-width of the specimens to ensure uniform loading in the transverse direction. The load was applied in displacement control at a rate of 3 mm/min. Six linear variable differential transducers (LVDTs) were used to instrument the loaded face of the specimen with data sampled at a rate of 16 to 20 Hz during specimen testing. Tests were terminated prior to collapse at a predicted load slightly less than that which would cause yielding of the reinforcement so as to prevent its sudden rupture.

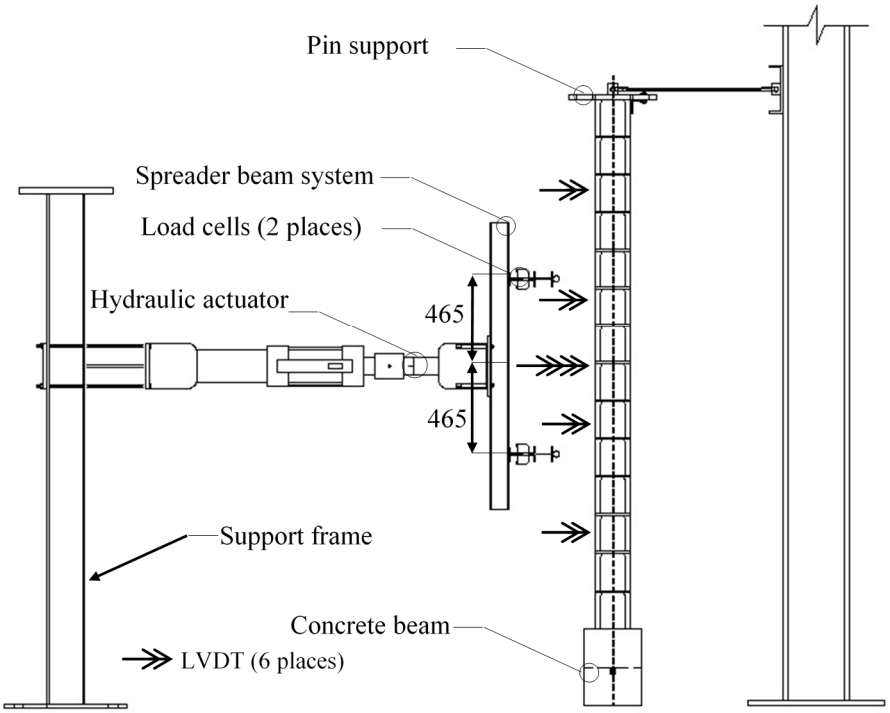

Figure 2: Loading Arrangement and Specimen Instrumentation

Figure 3: Top Support Assemblage

EXPERIMENTAL RESULTS

Table 1 summarizes the test results for the nine specimens including: the average initial force applied to the reinforcing bars in a given specimen, F_{pi} the initial cracking load, P_{cr}, the corresponding lateral deflection at mid-height of the wall, Δ_{cr}, and the maximum load applied to the wall, P_{max}, along with the corresponding lateral deflection at mid-height of the wall, Δ_{max}, at the point when testing was terminated. The sub-sections that follow describe the cracking and observed failure mode, and the load versus mid-height deflection response for all specimens.

Cracking and Observed Failure Mode

The cracking load reported in Table 1 was established from discontinuities identified in the load-deflection curves obtained for the specimens rather than the identification of cracks observed during testing. Nonetheless, the reported cracking loads for specimens that did not have their first course grouted (i.e. specimen series UB-U) were generally less than those specimens that were grouted (specimen series UB-G). The cracking loads for the UB-U specimen series were, however, greater than the 0.28 – 0.49 kN range reported for unreinforced specimens with otherwise similar geometry and test setup as reported by Miranda et al. [2].

The first visible crack in all specimens occurred on the unloaded wall face within the constant moment region between points of applied load or in the bed joint immediately above the upper load point, and so in a bed joint below one of block courses 7 to 11. A second flexural crack was then observed at the base of the wall on the loaded face. The mortar joint cracks became extremely wide (i.e. in the range of 15 to 30 mm for the crack within the constant moment region) at the point of maximum specimen loading as reported in Table 1, with a noticeable resulting inclination of the wall segments ranging from 2 to 5 degrees.

Load versus Mid-Height Deflection Response

Figure 4 shows the applied load versus mid-height deflection response for all nine specimens. Curves for all specimens exhibited a typical response consisting of three phases: (1) an initial, steep linear segment from the initiation of loading to the load corresponding to first cracking of the specimen, (2) a second linear segment with reduced slope following first cracking, and (3) a final segment with deteriorating slope as arching action becomes the predominant load-carrying mechanism.

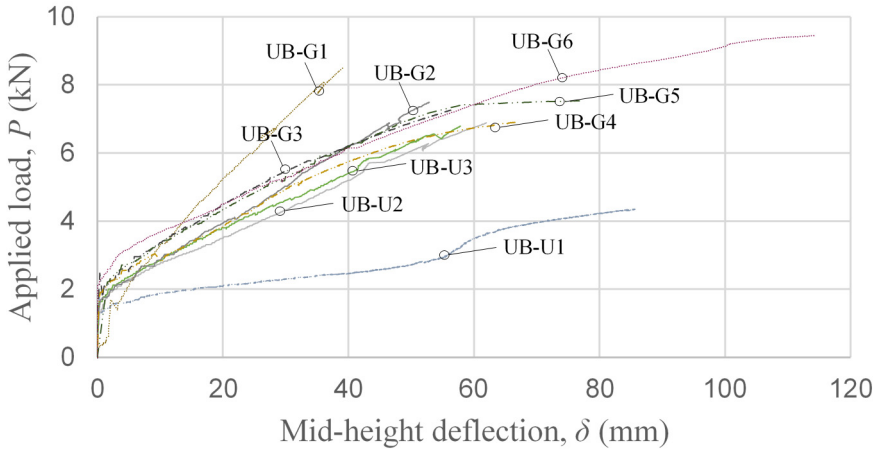

Figure 4: Experimentally Measured Applied Load versus Mid-Height Deflection

Figure 4 shows that the load resistance of Specimen UB-U1 was significantly less that that recorded for all other specimens at any measured mid-height deflection. It was observed during

testing of this specimen that the concrete grade beam was not properly clamped to the laboratory strong floor, resulting in visible rotation and an increase in the measured mid-height deflection at any magnitude of applied load. This specimen was therefore deemed to be a physical outlier and its results were excluded from the calculation of mean values for resulting cracking load and corresponding mid-height deflection. In contrast, there were no observations made that could explain the stiffer response obtained for Specimen UB-G1. Overall, Figure 4 shows that the load versus mid-height deflection response appeared to be insensitive to whether or not the first block course was grouted.

ANALYTICAL MODEL AND RESULTS

The applied load versus mid-height deflection of the specimens was estimated by modelling the wall assuming the formation of three hinges as shown in Figure 5(a): (1) in the bed joint between the concrete grade beam and the bottom of the wall (Point A), (2) at the top support (Point C^*), and (3) at mid-height of the wall (i.e. in the bed joint between the 7^{th} and 8^{th} block courses – Point B^*) regardless of the actual observed location of flexural cracking within the mid-height region of the specimen. The two resulting wall segments (i.e. bottom and top halves) were then assumed to undergo rigid body rotation and so remain straight and inextensible. It was also assumed that the steel rods used in the top support as pictured in Figure 3 were permitted to rotate but were not assumed to change length. The reinforcing bars in the wall were modelled as being elastic-perfectly plastic with a Young's modulus equal to 200 GPa and their as-tested yield strength of 542 MPa.

Once a value of lateral displacement at mid-height of the wall was selected, the displaced horizontal and vertical coordinates for the following points were established from trigonometry: the reinforcing bars at the six alignment plates; the centroids of the top and bottom wall segments; the centroid of the plate making up the support at the top of the wall specimen; and the reaction points as assumed at the bottom unloaded face of the wall, the contact point between the top and bottom wall segments as located on the loaded face at mid-height of the wall, and the centerline of the wall at its top.

The location of the reinforcing bars at each of the alignment plates, and at the top of the first course in the case of the UB-G specimen series, ultimately allowed for the calculation of the change in length of the bars and so the strain, stress, and force in the bars to be calculated; as well, the horizontal and vertical forces imposed by the bars on the plates, F_{six} and F_{siy}, respectively, could be calculated, where i is the number of the alignment plate from bottom to top of the specimen.

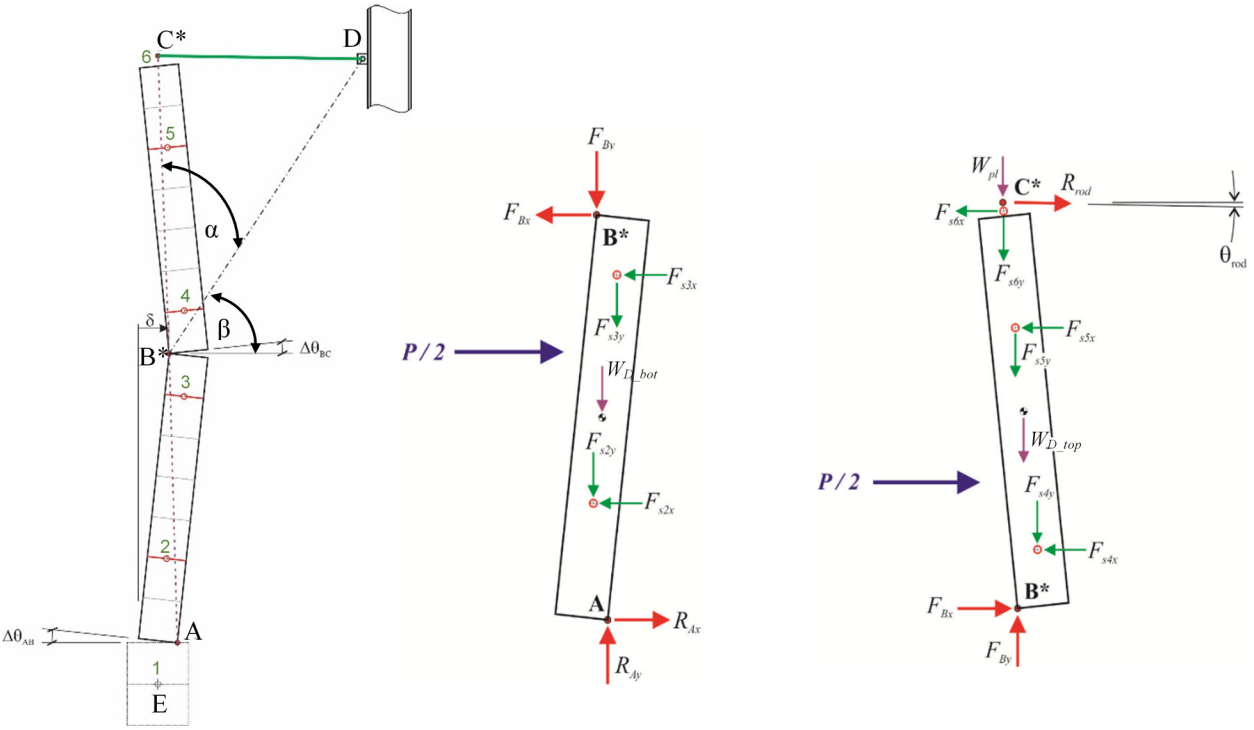

(a) (b) (c)

Figure 5: Analytical Model: (a) Assumed Specimen Geometry, (b) Free-Body Diagram of the Bottom Half of the Wall (shown for the UB-U specimen series), and (c) Free-Body Diagram of the Top Half of the Wall.

The evaluation of the deformed wall geometry further allowed for the evaluation of the change in length, and hence the combined resultant force R_{rod} in all rods that were part of the top wall support assembly.

Following the establishment of the displaced geometry of the wall specimen, the applied load P corresponding to the imposed lateral displacement at mid-height was determined by considering the free-body diagrams of the bottom (Figure 5(b)) and top (Figure 5(c)) wall segments. For this analysis, the self-weight of the bottom and top wall segments, W_{D_bot} and W_{D_top}, respectively, were assumed to act at the respective centroids the wall segments while in their displaced position. Similarly, the self-weight of the top support assembly, W_{pl}, determined to be equal to 0.95kN, was assumed to act at the longitudinal axis at the top of the wall specimen. The weight of the grout in the bottom block course (not shown in Figure 5(b)), as is applicable for the UB-G specimen series, was assumed to act at the centroid of this block course.

Repeating this procedure multiple times with varying magnitudes of the lateral displacement at mid-height of the wall allowed for the derivation of theoretical applied load versus mid-height deflection curve for any specimen.

Figure 6 shows a comparison of the experimental and analytically-derived applied load versus mid-height deflection curves for two specimens: one with the first course fully grouted (Specimen UB-G4), and one with all cells in all courses left ungrouted (Specimen UB-U3). This figure shows that the analytically derived curve matches reasonably well with that obtained experimentally at all levels of loading. A difference of 7.2 and -1.5% between the experimental and analytically obtained values of mid-height deflection at the maximum load for Specimens UB-G4 and UB-U3 resulted, respectively, with a positive value indicating that the analytical model over-estimated the applied load and a negative value showing that the analytical model under-estimated the applied load.

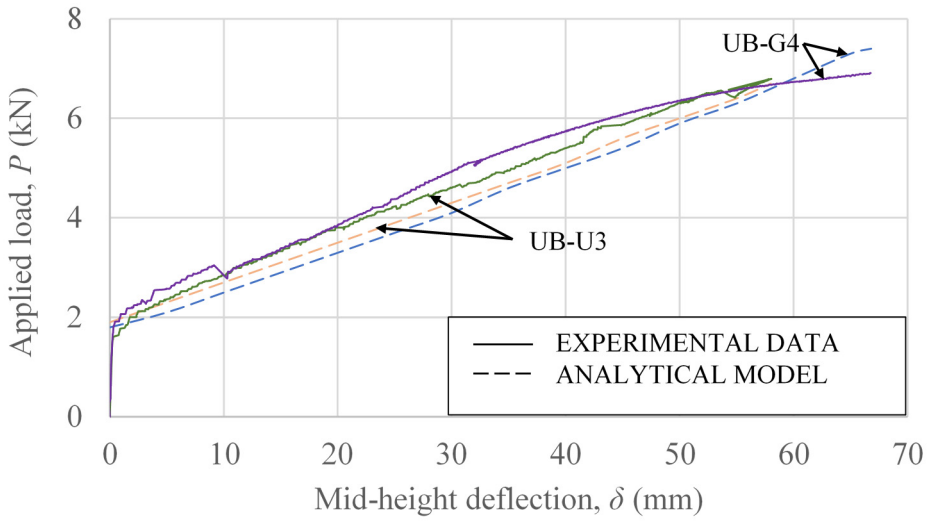

Figure 6: Comparison of Experimental and Analytical Load versus Mid-Height Deflection Results for Select Specimens

CONCLUSIONS

This paper presents the results of an experimental investigation consisting of nine concrete masonry block wall specimens, featuring conventional reinforcement placed in ungrouted cells, that were tested under four-point loading. Six of these specimens had all the cells in the first block course grouted while the remaining three specimens were completely ungrouted. All specimens were two and a half blocks wide and fourteen courses tall, and were constructed in running bond.

The following conclusions and observations were noted:

1. Cracking loads for specimens that did not have their first course grouted were generally less than those that were grouted, but still exceeded those reported for unreinforced specimens with otherwise similar geometry and loading conditions.
2. Mid-height deflections appeared to be insensitive to whether or not the first block course was grouted.

3. Specimens were modelled assuming rigid-body rotation following the formation of three hinges: one between the concrete grade beam and the bottom of the wall, one at the top support, and one in the constant moment region. The analytically-derived load-deflection response was found to match reasonably well with that obtained experimentally.

ACKNOWLEDGEMENTS

The research program was made possible by funding from the Saskatchewan Centre for Masonry Design (SCMD) and the Saskatchewan Masonry Institute (SMI). Financial support for the first author from the Ecuadorian Army (FTE) and the Government of Ecuador through the SENESCYT scholarship program are also gratefully acknowledged. Thanks are extended to Brennan Pokoyoway, laboratory technician, and mason Leon Gamble from BRXTON, for their assistance with the construction and testing of the specimens included in this experimental program.

REFERENCES

[1] Drysdale, R. G., Essawy, A.S. (1988). "Out-of-Plane Bending of Concrete Block Walls," *Journal of Structural Engineering*, 114(1): 121 – 133.

[2] Miranda, H., Feldman, L.R., and Sparling, B.F. (2016). "Feasibility of Using Unbonded Reinforcement in Concrete Block Walls." *Proc., 2016 CSCE Annual Conference*, London, ON, Canada, on USB.

[3] Dawe, J. L., Aridru, G. G. (1992). "Post-tensioned Concrete Masonry Walls Subjected to Uniform Lateral Loadings." *Proceedings of the 6th Canadian Masonry Symposium*, Saskatoon SK, Canada.

[4] Devalapura, R. K. (1995). Development of Prestressed Clay Brick Masonry Walls. Ph.D. thesis, University of Nebraska, Lincoln, NE, United State of America.

[5] Harton, R.T., Tadros, M.K., "Deflection of Reinforced Masonry Members," ACI Structural Journal, 87(4): 453-463.

[6] Graham, K. J. and Page, A. W. (1995). "The Flexural Design of Post-tensioned Hollow Clay Masonry." *Proceedings of the 7th Canadian Masonry Symposium*, Hamilton, ON, Canada.

[7] Phipps, F.N. (1993). "The Principles of Post Tensioned Masonry Design." *Proceedings of the 6th North American Masonry Conference*, Philadelphia, PA, United States of America.

[8] Bean Popehn, J.R., Schultz, A.E., and Drake, C.R. (2007). "Behavior of Slender, Posttensioned Masonry Walls Under Transverse Loading," *Journal of Structural Engineering*, 133(11): 1541 - 1550

[9] American Society for Testing and Materials (ASTM) (2015). *ASTM A1064/A1064M-15: Standard Specification for Carbon-Steel Wire and Welded Wire Reinforcement, Plain and Deformed, for Concrete*, ASTM, West Conshohocken, PA, United States.

[10] Canadian Standards Association (CSA) (2004). *CAN/CSA S304.1-04 (R2010) Design of Masonry Structures*, Canadian Standards Association, Mississauga, ON, Canada.

[11] American Society for Testing and Materials (ASTM) (2015). *ASTM A370-15: Standard test methods and definitions for mechanical testing of steel products*, ASTM, West Conshohocken, PA, United States.

[12] Canadian Standards Association (CSA) (2008). *CAN/CSA A3000-08 Cementitious Materials Compendium*, Canadian Standards Association, Rexdale, ON, Canada.

[13] Udey, A. (2014). Realistic Wind Loads on Unreinforced Masonry Walls, M.Sc. thesis, University of Saskatchewan, Saskatoon, SK, Canada.